Supplementary information

Sodium chloride-assisted CVD enables controlled synthesis of large single-layered MoS$_2$

Ting Li[a,b], Chong Zhang[a,c], Yali Cai[a,c], Wenfeng Yue[a], Jie Liu[a], Chuanwei Huang[b], Quansheng Guo[c], Tingting Jia[a,c]*, Shuhui Yu[a]

[a] Shenzhen Institute of Advanced Electronic Materials, Shenzhen Institute of Advanced Technology, Chinese Academy of Sciences, Shenzhen 518055, China

[b] School of Materials Science and Engineering, Shenzhen University, Shenzhen 518055, China

[c] School of Materials Science and Engineering, Hubei University, Wuhan 430062, China

[d] School of Instrumentation Science and Engineering, Harbin Institute of Technology, Harbin 150001, China

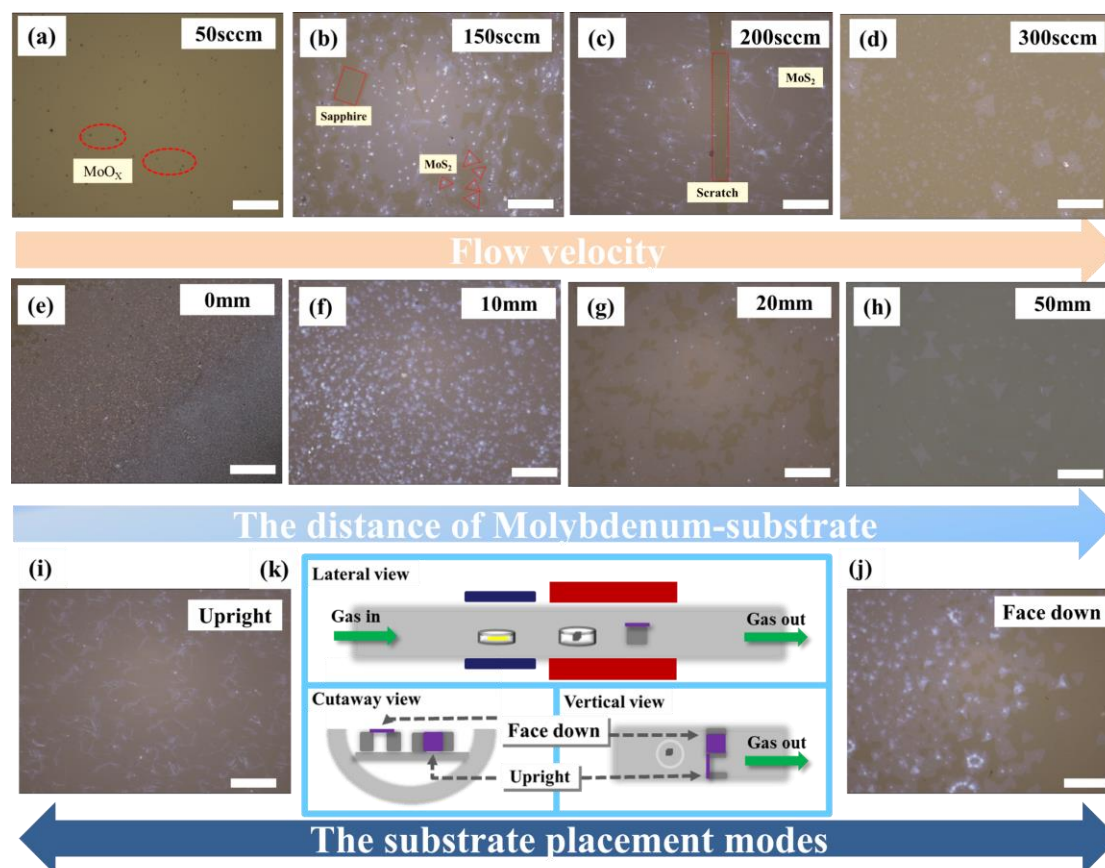E-mail address: jia tingting@hubu.edu.cn

Fig S1. The morphology of MoS$_2$ growth on sapphire substrate influenced by (a-d) the gas flow rates, (e-h) the distance between MoO$_3$ with the substrate and (i-j) the substrate placement modes.

As seen in Fig.S1 (a-d), with the rise of gas flow rates from 50-200 sccm (Standard cubic centimeter per minute), the size and quality of the MoS_2 nanosheet changes remarkably. Combined with our data results, when the velocity of N_2 is too low ($\leq$ 100 sccm), the N_2 flow in the tubular furnace chamber is not enough to quickly bring the S steam from the low temperature region to the high temperature zone, resulting in the high concentration of MoO_x near the substrate and finally deposited on the surface of the substrate[2]; Similarly, when the N_2 flow rate is too high ($\geq$ 200 sccm), the S vapor does not have time to react with MoO_3, the vulcanization process is not complete and the intermediate products can be obtained. Only when the velocity of carrier gas is about 200 sccm, a good reaction can take place between the precursors and high quality MoS_2 can be formed and deposited on the substrate surface.

The chemical reaction equation for the conversion from MoO_3 to MoS_2 in N_2 atmosphere is as follows :

$$2\ MoO_3 + 7\ S \rightarrow 2\ MoS_2 + 3\ SO_2 \qquad (1)$$

$$MoO_3 + x/2\ S \rightarrow MoO_{3-x} + x/2\ SO_2 \qquad (1)$$

$$MoO_{3-x} + (7-x)/2\ S \rightarrow MoS_2 + (3-x)/2\ SO_2 \qquad (2)$$
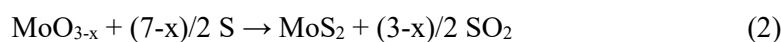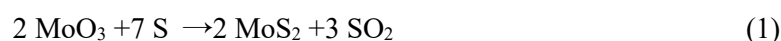
Fig. S1 (e-h) shows that the optical microscopy images of the MoS_2 growth state on the substrate surface when the MoO_3 is placed at different distances with the substrate, which is important influence on the growth of MoS_2. When the distance is small (Fig S1(e, f)), the concentration of MoO_3 vapor is extremely high, and the kinds of materials deposited on the substrate surface are complex, and it is easier to grow multi-layer MoS_2. Moreover, when the distance is too far (Fig.S1(h)), it will cause uneven MoO_3 vapor concentration, and it is difficult to control the growth of MoS_2. In our experiments, we found that when the distance is 20 mm, it is easier to grow large area monolayer MoS_2.

In our experiments, it is found that the optimum gas flow rates and placement distance are around 200 sccm and 20 mm, respectively. Certainly, it is worth noting that practical considerations will also cause the experimental results to differ. The fundamental reason is that the optimized gas flow rates and placement distance will increase the time of raw material reaction and enhance the size and quality of the MoS_2 nanosheet remarkably.
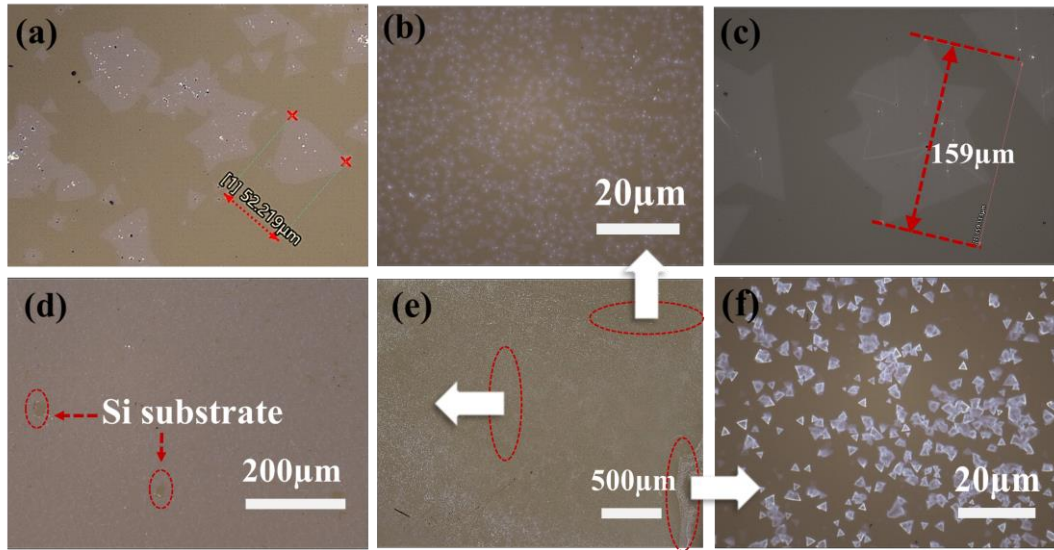
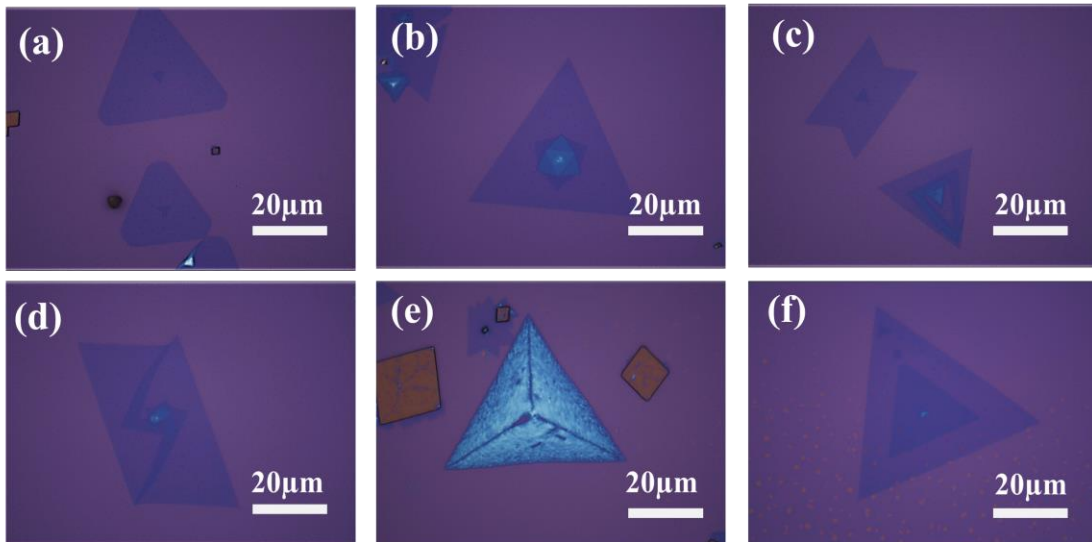Fig S2. (a-f) The same substrate surface has different growth states at different positions.

Fig. S3. (a-f) The morphology of MoS_2 grown on SiO_2/Si shows many kinds, such as

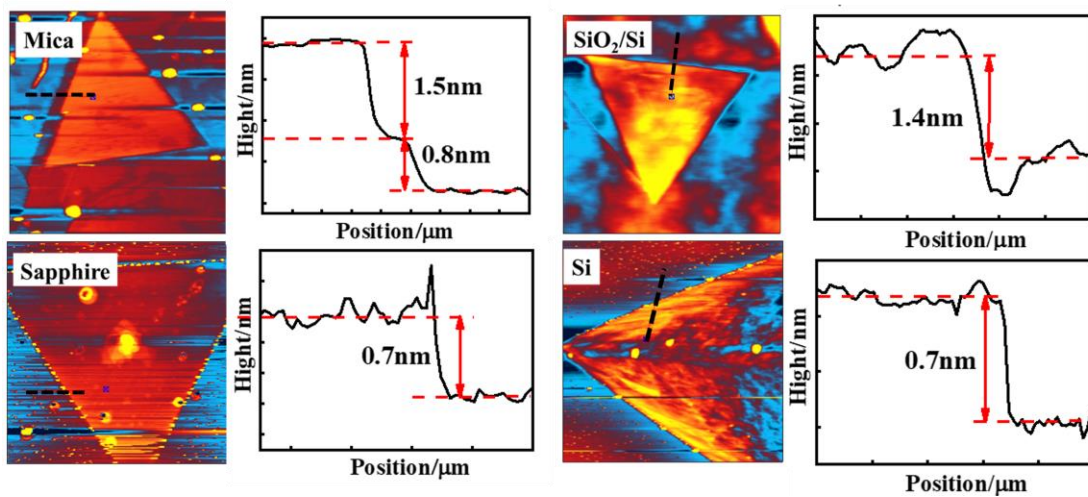dendritic, triangular, and butterfly shapes

Fig. S4. In the same environment, the thickness of MoS_2 nanosheets grown on four different substrate surfaces was measured. The mica surface showed a distinct step-like morphology, and height measurements confirmed the presence of three layers in the crystal domain. MoS_2 domains observed on SiO_2/Si substrates appeared relatively smooth, while those on sapphire and Si substrates were observed to be monolayers with a thickness of approximately 0.7nm. The MoS_2 grown on Si exhibited more pronounced sawtooth patterns, while the boundaries of the MoS_2 grown on sapphire showed small particle aggregation, suggesting the presence of unreacted MoO_{3-x} or MoO_xS_{2-y} nanoparticles.
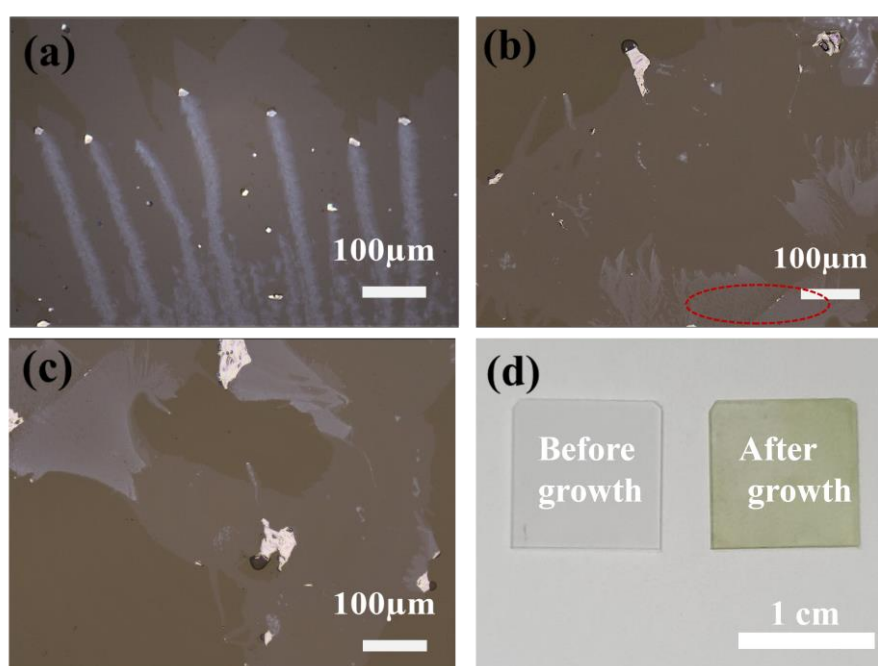
Fig. S5. Pre-treatment of the sapphire substrate with a NaCl solution at a concentration of 25 mg/mL resulted in the morphology of the grown MoS_2 nanosheets shown in (a-c). Clearly demonstrating the vapor-liquid-solid (VLS) reaction [3] model on the substrate surface, with monodomain sizes of approximately 1 mm. (d) Shows a comparison of the substrate before and after the growth of MoS_2 on a sapphire substrate, where MoS_2 appears pale yellow to the naked eye, indicating growth throughout the entire substrate surface.
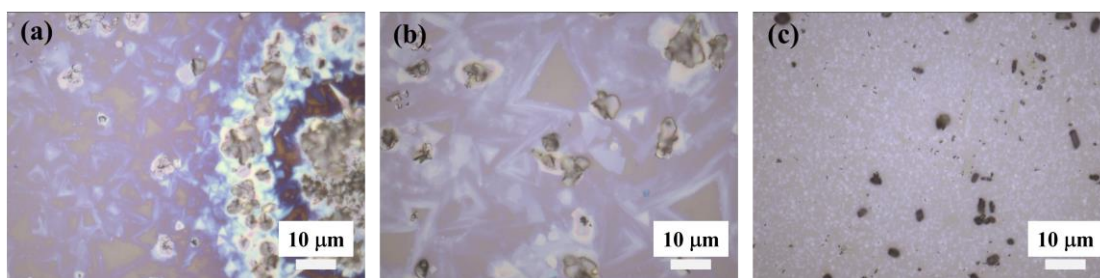
Fig. S6. Pre-treatment of the Si substrate with the same concentration (25 mg/mL) of NaCl solution for 5 cycles achieved a high concentration pre-treatment target, followed by CVD growth. The growth conditions at different positions on the substrate surface are shown in (a-c). A high concentration pre-treatment implies the introduction of more ion suspension bonds on the substrate surface, resulting in decreased controllability of the growth state and an increased probability of contamination of the grown MoS_2 nanosheets by impurities.
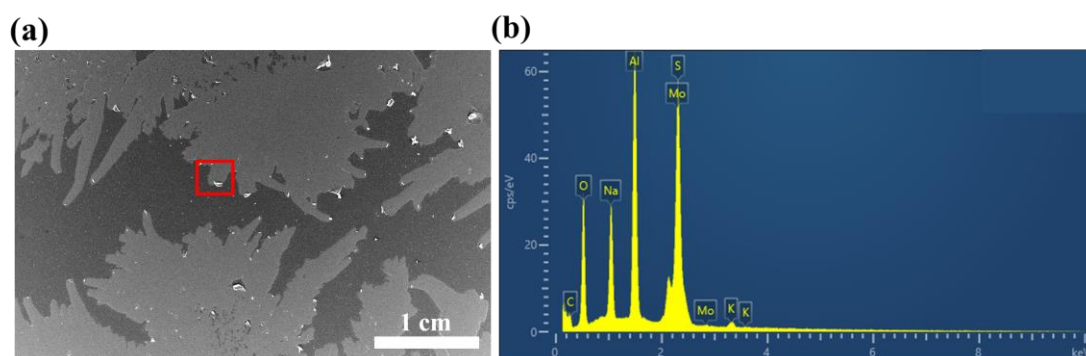
Fig. S7. (a) SEM image of MoS_2 grown on a sapphire substrate surface after NaCl solution pre-treatment, and (b) EDS elemental distribution map at the red box position in (a).

Table S1. The chemical element content is shown in Fig. S7(b).

Chemical element	Wt%	At%
C	4.32	9.61
O	21.63	36.12
Na	8.10	9.41
Al	19.79	19.60
S	21.30	17.76
K	1.41	0.96
Mo	23.45	6.53
Total	100.00	100.00
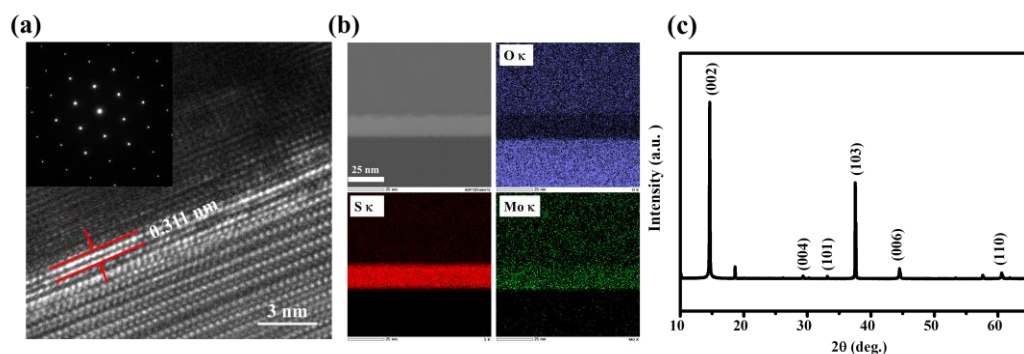
Fig S8. (a) High-resolution TEM image of a single MoS$_2$ nanosheet. The red circles in the outline the six-fold-symmetric diffraction spots. The labelled plane in a is indexed to be the (002) plane, with 0.311 nm lattice spacing. (b) EDS image at the cross-section position, with the positions of elements such as O, S, and Mo labeled. (c) XRD characterization of the same batch of samples.

(a)

```
Thin Film Standardless   Standardless Quantitative Analysis
Fitting Coefficient : 0.5396
Element        (keV)  Mass%    Counts    Sigma  Atom%  Compound  Mass%  Cation       K
  C K          0.277   6.59  10087.46    0.07   45.23                             1.1341
  O K          0.525   1.82   6569.42    0.04    9.37                             0.4807
  Al K         1.486   1.46   9024.75    0.04    4.45                             0.2803
  S K          2.307   0.58   3291.63    0.05    1.50                             0.3087
  Ga K         9.241   0.68   1744.34    0.05    0.81                             0.6780
  Mo K        17.441   3.14   1956.50    0.13    2.70                             2.7844
  W M          1.774   1.04   2102.08    0.08    0.46                             0.8556
  Au M (Ref.)  2.120  84.70 147115.55    0.44   35.47                             1.0000
  Total               100.00                    100.00
```

(b)

```
Thin Film Standardless   Standardless Quantitative Analysis
Fitting Coefficient : 0.5449
Element        (keV)  Mass%    Counts    Sigma  Atom%  Compound  Mass%  Cation       K
  C K          0.277   6.00   8907.20    0.07   41.96                             1.1341
  O K          0.525   1.89   6629.22    0.04    9.94                             0.4807
  Al K         1.486   1.43   8588.80    0.04    4.45                             0.2803
  S K          2.307   1.00   5474.72    0.05    2.63                             0.3087
  Ga K         9.241   0.69   1724.78    0.05    0.84                             0.6780
  Mo K        17.441   4.92   2976.20    0.16    4.31                             2.7844
  W M          1.774   0.98   1919.48    0.08    0.45                             0.8556
  Au M (Ref.)  2.120  83.08 139860.41    0.44   35.43                             1.0000
  Total               100.00                    100.00
```

(c)

```
Thin Film Standardless   Standardless Quantitative Analysis
Fitting Coefficient : 0.5407
Element        (keV)  Mass%    Counts    Sigma  Atom%  Compound  Mass%  Cation       K
  C K          0.277   6.55  10680.57    0.07   46.24                             1.1341
  O K          0.525   1.51   5825.34    0.04    8.02                             0.4807
  Al K         1.486   1.09   7189.61    0.03    3.42                             0.2803
  S K          2.307   0.52   3089.02    0.04    1.36                             0.3087
  Ga K         9.241   0.74   2016.80    0.05    0.90                             0.6780
  Mo K        17.441   3.18   2110.86    0.13    2.81                             2.7844
  W M          1.774   1.10   2371.50    0.08    0.51                             0.8556
  Au M (Ref.)  2.120  85.32 157826.08    0.43   36.74                             1.0000
  Total               100.00                    100.00
```
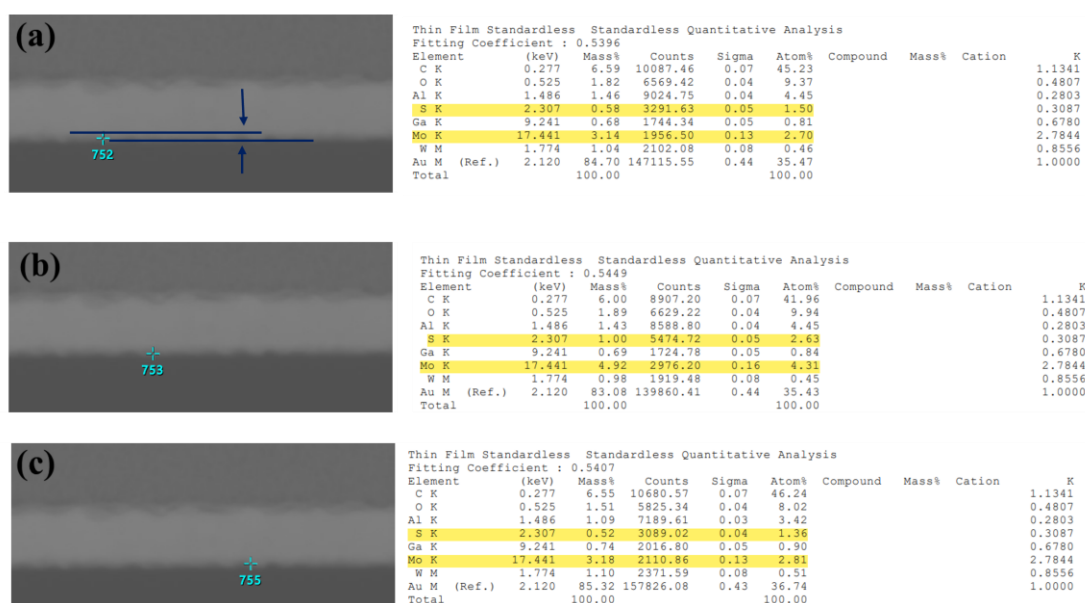
Fig S9. (a-c) EDS data summary and comparison of Mo and S element contents marked at three different positions.

Due to the hardness of sapphire, the sample was sent for FIB sectioning before TEM imaging. To clearly locate the target sample during the sectioning process, gold deposition was performed on the sample surface in advance, with a thickness of approximately 6-10 nm. This also posed some difficulties in observing the MoS$_2$ sample. Therefore, in the observed cross-section, only a thin layer (~1 nm) close to the sapphire substrate is the MoS$_2$ sample.

REFERENCES:

[1] Li X L andLi Y D Formation of MoS$_2$ inorganic fullerenes (IFs) by the reaction of MoO$_3$ nanobelts and S 2003 Chemistry 9 2726-31

[2] Weber T; Muijsers J C; Van Wolput J H M C; Verhagen C P J andNiemantsverdriet J W Basic Reaction Steps in the Sulfidation of Crystalline MoO$_3$ to MoS$_2$, As Studied by X-ray Photoelectron and Infrared Emission Spectroscopy 1996 The Journal of Physical Chemistry 100 14144-14150

[3] Li, S. et al. Vapour–liquid–solid growth of monolayer MoS$_2$ nanoribbons. Nat.Mater. 17, 535–542 (2018).